5 CT Angiography in the Assessment of Intracranial Vessels

Toshinori Hirai, Yukunori Korogi, Mutsumasa Takahashi, and Yasuyuki Yamashita

CONTENTS

5.1 Introduction

Computed tomographic angiography (CTA), a rapidly evolving field in CT imaging, is a noninvasive tool for visualizing blood vessels. The acquisition of thin-slice continuous images of the blood vessels, in which contrast material is used, is necessary to create three-dimensional (3D) reformations of the intracranial vessels. This technique offers a greater capability for identification and characterization of intracranial vascular diseases. While magnetic resonance angiography (MRA) also allows accurate depiction of intracranial vascular diseases and may be used as a screening method, CTA may be used as a further definitive evaluation or preoperative evaluation. Compared with single-detector helical CT, multidetector-row CT improves temporal and spatial resolutions, allowing nearly isotropic images with large volumes such as the entire bed of intracranial vascular structures. Since CTA has some limitations such as inferior spatial and temporal resolutions to digital subtraction angiography (DSA), this technique may not be able to replace DSA in general.

This article aims to illustrate the state-of-the-art techniques of CTA and three-dimensional reconstruction, as well as their application in the evaluation of intracranial lesions.

5.2 Data Acquisition Techniques

3D CTA of the intracranial vessels can be performed with conventional single-detector helical CT or multidetector-row CT scanners. Multidetector-row CT scanners have several advantages over single-detector helical CT in general. These include improved temporal resolution, improved spatial resolution in the *z*-axis, decreased image noise, and longer anatomical coverage [1]. Multidetector-row CT scanners acquire data more quickly, allowing isotropic or nearly isotropic images with large volumes such as the entire vascular structures of the head. When the vascular diseases are in a limited region such as the circle of Willis, the advantages of multidetector-row CT may be small because the image quality of the vessels in a limited area is usually sufficient even by single-detector helical CT.

According to the location of the vascular lesions or suspected vascular lesions on CT, MRI, or MRA, the scanning volume of CTA is usually determined in each case. When the location of lesions is at the circle of Willis or supratentorial region, the volume scanning usually begins at the level of the sellar floor

T. Hirai, MD; Y. Korogi, MD; Y. Yamashita, MD
Department of Radiology, Kumamoto University School of Medicine, 1-1-1 Honjo, Kumamoto 860-8556, Japan
M. Takahashi, MD
Kumamoto University School of Medicine, International Imaging Center, 1-2-23 Kuhonji, Kumamoto 862-0976, Japan

and is continued cranially. When the lesions are multiple or unknown, the volume scanning may begin at the level of the foramen magnum and be continued cranially. Multidetector-row CT scanners are preferable for wider anatomical coverage such as the entire vascular structures from the aortic arch to the intracranial vessels.

In four-detector-row multisection helical CT for the head region, volume data may be acquired in 10–20 s using a slice thickness of 1.0–1.25 mm and a table speed of 3.0–3.75 mm/s (200 mAs; 120 kV); the scanning volume may be 30–60 mm with a 512×512 matrix (Table 5.1). The actual acquired voxel size was 0.47×0.47×0.5 mm. With 16-detector-row multisection helical CT, the scanning speed is 4 times faster than that of four-detector-row multisection helical CT.

5.3 Methods of Contrast-Agent Administration

In order to obtain high-quality CTA images, high concentration of contrast material in the vessels is necessary. Technique-related factors such as contrast material volume and concentration, rate of injection, and type of injection and patient-related factors such as body weight may affect CT contrast enhancement [2, 3]. When the attenuation of the intracranial vessels is usually more than or nearly 300 HU, the image quality of 3D or multiplanar reformations (MPR) are usually satisfactory. Intravenous contrast-agent administration is generally performed in conventional intravenous CTA, while contrast agent is intraarterially administrated in intraarterial CTA

In intravenous contrast-agent administration, there are three methods available: a fixed scan delay technique, a test bolus injection technique, and an automated bolus-tracking technique (Table 5.2). A total of 100–150 ml of nonionic contrast material (300 mg I/ml) is usually injected into the antecubital vein with a flow rate of 2.0–4.0 ml/s by using a power injector.

A fixed scan delay (15–45 s) after the initiation of intravenous contrast injection has been used commonly to obtain the intracranial arterial phase, without taking into account differences in transit time of contrast material [4–7]. This technique has a potential of missing the optimal timing of intracranial arterial phase. To avoid the situation, a larger volume of contrast material may be needed.

A test bolus injection technique is a method to measure the time between the initiation of intravenous contrast injection and the arrival of contrast material in the vessels interested [8, 9]. This technique requires additional volume of contrast material and monitoring the arterial enhancement by periodical CT scanning. Based on this result, a scan delay is determined.

An automated bolus-tracking technique is another method to obtain the optimal arterial phase [10, 11]. Placement of region of interest (ROI) and choice of a threshold of arterial enhancement are needed for radiologists or technologists. The ROI may be placed in the carotid artery near the skull base. Then this technique consists of automated ROI measurement in the selected artery during low-dose scans obtained every few seconds after contrast medium injection. When arterial enhancement reaches the threshold, the spiral scan is initiated.

Table 5.1 Acquisition parameters for intracranial CTA

Detectors of CT	Collimation (mm)	Table speed (mm/s)	Slice thickness/ reconstruction interval (mm)	Scanning time (s)
Single detector	1	1–1.5	1/0.5–1	30–40
Four-detector	1–1.25×4	3–3.75	1–1.25/0.5–0.8	10–20

Table 5.2 Intravenous contrast-agent administration for intracranial CTA

Techniques of contrast-agent administration	Volume of contrast agent (ml)	Monitoring arterial enhancement	Placement of region of interest	Reliability
Fixed scan delay	100–200	No	No	Relatively low
Test bolus injection	100–150	Yes	No	High
Automated bolus tracking	100	Yes	Yes	High

The technique of contrast-agent administration may be determined by the capability of CT unit and radiologist's preference. Unlike intravenous contrast-material injection in conventional CTA, intraarterial CTA is a relatively invasive examination and is performed with a combined angiography and CT unit [12]. This method has theoretical advantages compared with intravenous contrast-agent administration, because a higher concentration of contrast material can be obtained in the intracranial artery without considering the appropriate timing of injection, and a smaller amount of contrast material can be used. When evaluating intracranial aneurysms, a total of 16–24 ml of diluted contrast agent, 4–6 ml of nonionic contrast material (300 mg I/ml) diluted with triple volume of saline (12–18 ml), is injected into the carotid artery at a flow rate of 0.6–0.8 ml/s by using a power injector [12].

5.4 Postprocessing and Display Techniques

There are various display techniques in CTA. They include axial, MPR, maximum-intensity projection (MIP), surface rendering, volume rendering, and virtual endoscopy methods. Although all these techniques are valuable in displaying CTA data, it has not been established which technique or which combination of the techniques is the best or better method for identification and characterization of intracranial vascular diseases.

Axial and MPR images have basic information from the volume data for the intracranial vessels. They enable the evaluation of relationship between calcification or bony structure and intracranial vessel lumens. The assessment of the intracranial vessels is not able to perform with 3D reformatted images alone [11]. In the evaluation of the vessels in the skull base, axial and MPR images are essential (Fig. 5.1). The curved MPR method may be useful for the assessment of the tortuous vessels and the vessels surrounded by bony structures [13].

MIP is a widely used method for CTA and MRA (Fig. 5.2b). The single layer of the brightest voxels is displayed without use of attenuation threshold. When arterial luminal attenuation is smaller than calcification, calcification can often be differentiated from arterial lumens. Although the attenuation information is maintained, the depth information is lost. Therefore, intracranial vessel structures are superimposed as two-dimensional projection angiograms.

The surface rendering method shows the first layer of voxels within defined thresholds, that is, the visualization of the surface of all structures. The caliber of the intracranial artery varies depending on the thresholds selected. This may lead to a slight overestimation of the vessel structures. Unlike MIP, the attenuation information is lost but the depth information is preserved. Calcification cannot be separated from arterial lumens but the spatial relationship between the vessels is understood.

3D images with volume rendering have a number of theoretical advantages over MIP and surface rendering [14, 15] (Figs. 5.1, 5.2, 5.3). Groups of voxels within defined attenuation thresholds are chosen and relative

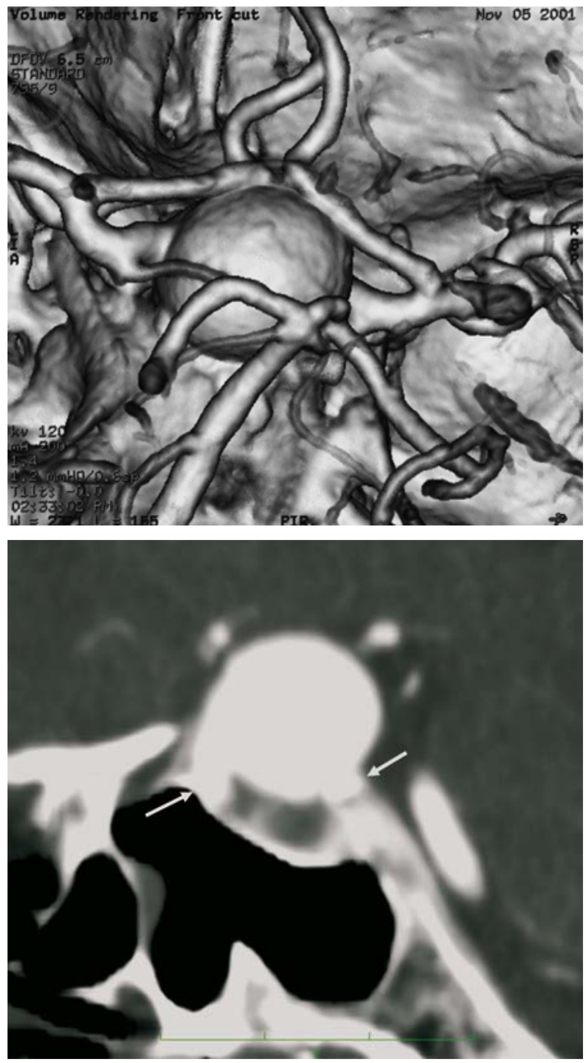

a b

Fig. 5.1a,b A 60-year-old woman with an unruptured giant aneurysm of the left internal carotid–ophthalmic artery. **a** Volume-rendered computed tomography angiogram (CTA) from behind and above demonstrates a giant aneurysm extending to the anterior communicating artery. **b** Multiplanar reconstruction image of CTA shows the relationship between the giant aneurysm and the left internal carotid artery (arrows).

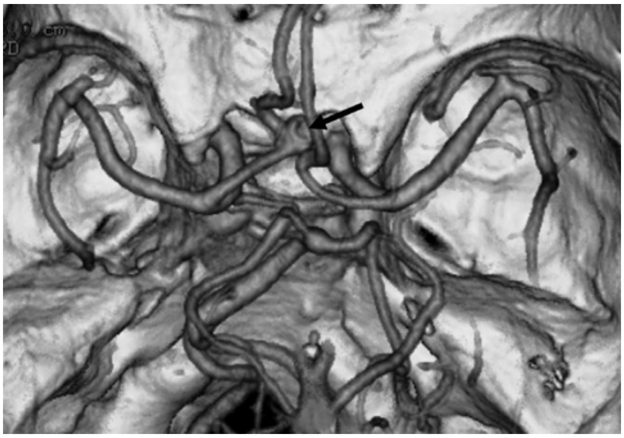

a

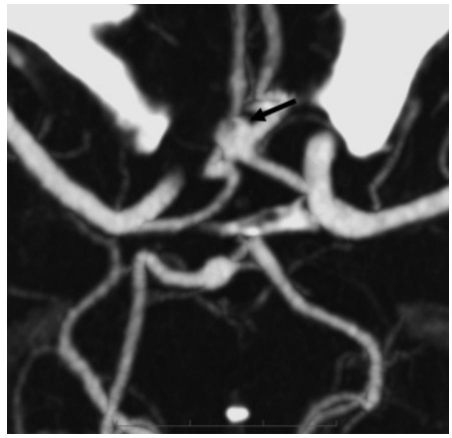

b

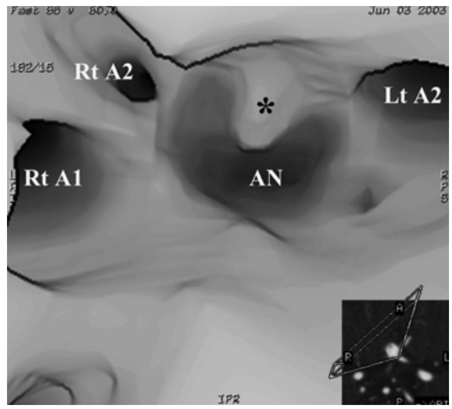

c

Fig. 5.2a-c A 61-year-old man with an unruptured aneurysm of the anterior communicating artery. **a** Volume-rendered CTA from above shows an aneurysm at the anterior communicating artery (*arrow*). **b** Maximum-intensity projection image of CTA from above depicts an aneurysm at the anterior communicating artery, but the relationship between the aneurysm (*arrow*) and the adjacent arteries is not clearly understood. **c** Virtual endoscopy from the left A1 segment shows thrombus (*star*) within the aneurysm (*AN*) and the adjacent arteries. *Rt A1*, right A1 segment; *Rt A2* right A2 segment; *Lt A2*, left A2 segment

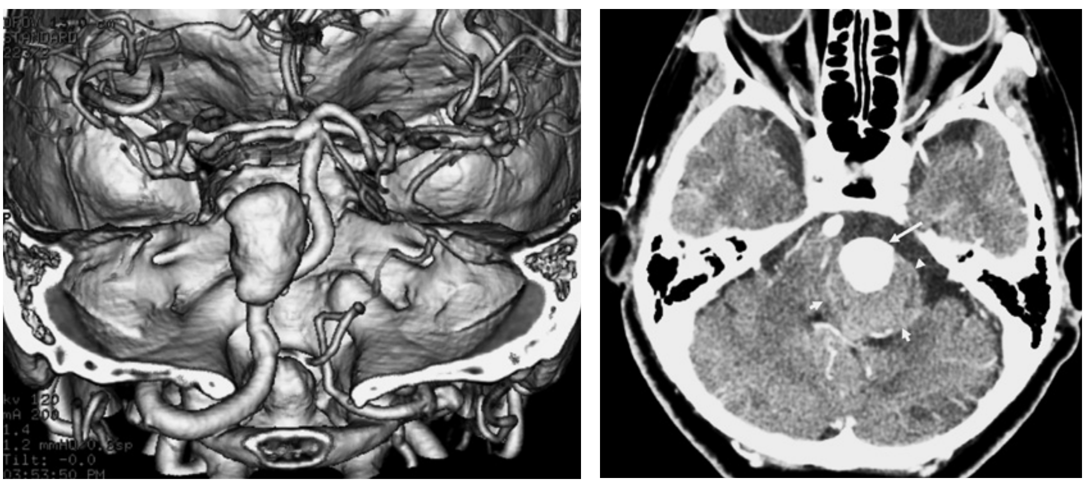

a b

Fig. 5.3a,b A 67-year-old woman with an unruptured giant aneurysm of the left vertebral artery. **a** Volume-rendered CTA from behind and above shows a giant aneurysm of the left vertebral artery. Thrombus in the aneurysm is not depicted. **b** Axial source image of CTA shows partial thrombus (*arrowheads*) within the aneurysm. The lumen of the aneurysm is located anteriorly (*arrow*).

Fig. 5.4a–d A 76-year-old man with severe stenoses of the left vertebral artery. **a** Anteroposterior digital subtraction angiogram of the left vertebral artery shows severe stenoses and segmental dilatation in the intracranial segment of the left vertebral artery (*arrows*). **b** MRA image also depicts severe stenoses and dilatation in the left vertebral artery (*arrows*). **c** Volume-rendered CTA image from behind shows aneurysm-like dilatation of both vertebral arteries (*arrows*), which correspond to the calcification of the vessel wall. **d** Axial source image of CTA demonstrates no apparent lumen in the stenotic artery because of circumferential calcification. (Adapted from [11]) voxel attenuation is conveyed by means of a gray scale, which yields images that are more accurate than those with surface rendering [15]. The volume-rendered images maintain the original anatomical spatial relationships of the 3D angiography data set and have a 3D appearance, facilitating interpretation of vascular interrelationships, which is limited with MIP images [15]. The quality of volume-rendered 3D angiography is essential in the imaging of the intracranial vasculature, especially vascular lesions such as aneurysms. Although the volume-rendering technique has much larger data volume than MIP and surface-rendering techniques, new computer processing and display systems do not limit its practical and versatile use.

Virtual endoscopic images can be obtained by a perspective volume-rendering method [16, 17] (Fig. 5.2c). With this method, the volume data are rendered from a point source at finite distance to approximate the human visual system.

5.5 How to Analyze Images

The axial or MPR images are always analyzed in conjunction with the corresponding 3D images because of the potential for misinterpretation inherent in the evaluation of 3D images alone.

Calcifications in the arterial wall are the limiting factor of 3D images owing to the inability to separate mural calcification and intramural contrast material (Fig. 5.4). MIP may allow the visualization of both calcification and arterial lumen. To minimize this limi-

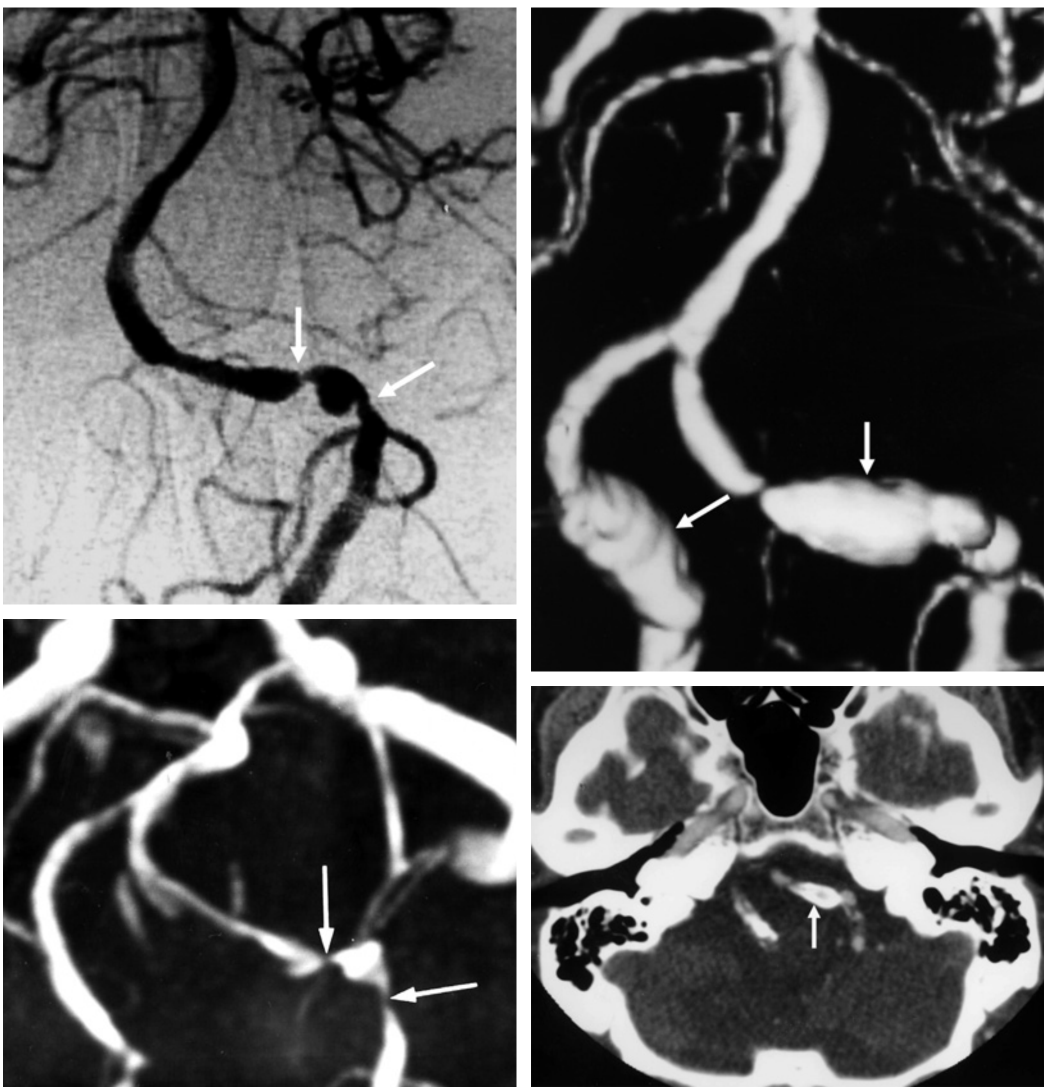

tation, analysis in conjunction with the axial source or MPR images is necessary. Dense circumferential calcification of the arterial wall may cause artifacts that interfere with the evaluation of the arterial lumen on axial or MPR images of CTA [11].

In the skull base region, CTA often fails to identify the lumen of the internal carotid artery within the cavernous sinus, because the cavernous sinus is enhanced [11]. When the density of the arterial segment is greater than that of the cavernous sinuses, the MPR or curved MPR images can usually assess the lumen of the arterial segment. However, when the cavernous sinuses are equally enhanced relative to the carotid artery, this arterial segment cannot be differentiated from the venous structure.

Careful evaluation for the superimposition of the bone and venous structures is needed when the intracranial arteries are assessed. The basal vein of Rosenthal may overlap with the middle and posterior cerebral arteries. The skull base structures such as the anterior and posterior clinoid processes contact with the internal carotid artery. This overlapping of the structure is usually resolved by careful evaluation of continuity of the vessels using MPR and axial source images.

To eliminate the skull base bone, subtraction methods have been developed [18–20] (Fig. 5.5). Although the techniques allow the visualization of the internal carotid artery without bony structures, this issue has not been completely resolved.

5.6 Comparison with Other Modalities

MRA is another noninvasive imaging modality. This technique includes time-of-flight (TOF) and phase-contrast methods. In the evaluation of intracranial vessels, TOF MRA is widely used because of its better spatial resolution and shorter examination time. On TOF MRA, 3D images are preferable for intracranial arteries and 2D images are often used for intracranial venous structures. In the assessment of the cervical carotid arteries, contrast-enhanced MRA has become a more accurate diagnostic method than conventional MRA [21].

With regard to depiction of the intracranial vessels, CTA has several advantages compared with TOF MRA. Acquisition time for CTA is faster than for TOF MRA. Since patients may have claustrophobia and need patience for longer examination time for MRI, the patient acceptance of the examination is much higher for CTA. CTA provides the information about

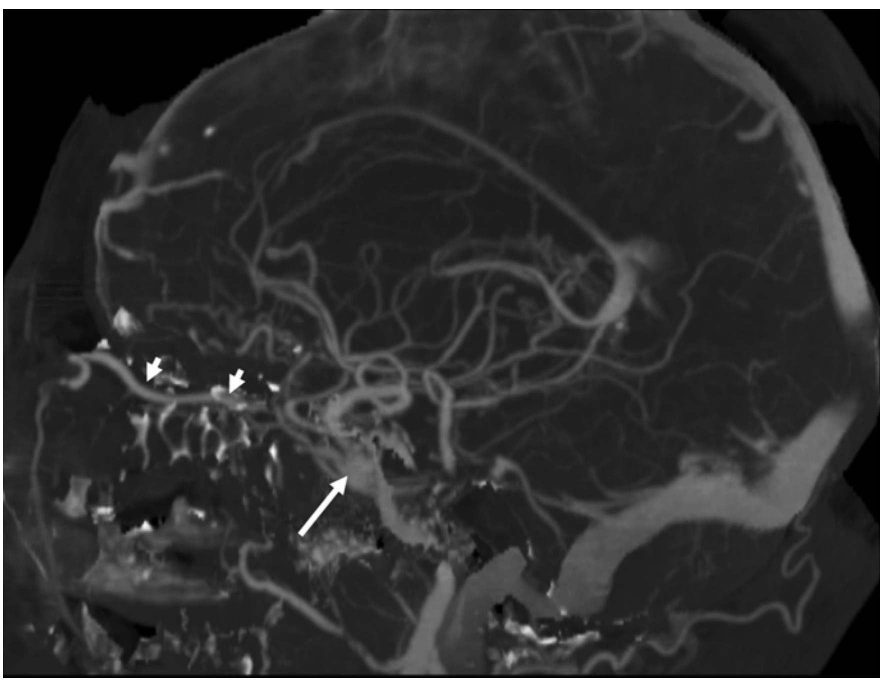

Fig. 5.5 An 81-year-old woman with dural arteriovenous fistula at the left cavernous sinus. Selective maximum-intensity projection image of CTA with bone subtraction shows the left cavernous sinus (*arrow*) and the dilatation of the left superior orbital vein (*arrowheads*). Bony structures are partially visualized because of incompleteness of subtraction.

the relationship between the vessels and the bony structure, while TOF MRA does not.

TOF MRA has several limitations in identifying and grading stenoses. First, the vessels that lie near the sphenoid sinus are subject to artifactual narrowing or nonvisualization owing to the large susceptibility gradient present in this area [22], although this issue is not so problematic with recent MRI units, resulting in a superiority of MRA over CTA in this region [11]. The artifacts may be minimized with the development of MRA sequences. Second, acceleration of flow in the carotid siphon and loss of laminar flow and resultant intravoxel dephasing can also contribute to artifactual signal loss in the C2 and C3 portions of the internal carotid artery, making it difficult to evaluate narrowing of this segment of the vessel [22] (Fig. 5.6). Third, MR angiograms of severely stenotic vessels often show an apparent discontinuity in a vessel. The flow void results from intravoxel spin dephasing and the acceleration of spins through the area of stenosis [23]. These artifacts may result in overestimation of stenosis on MRA alone. These disadvantages are not seen on CTA, because CTA shows the vessel lumen filled with contrast material such as DSA.

Disadvantages of CTA include the need for exposure to ionizing radiation, injection of iodinated contrast material, optimization of imaging delay time, and careful evaluation for superimposition of the bone and venous structures. Since CTA has inferior spatial resolution to DSA and does not provide information about intracranial hemodynamics, CTA cannot replace DSA in general. The amount of radiation exposure during CTA is without doubt greater than that during conventional CT but is significantly less than that during DSA [7]. The amount of ionizing radiation may not be an important concern in the predominantly older patient population. Iodinated contrast agents must be used with caution in patients with serious risk factors, such as renal insufficiency, congestive heart failure, or hypersensitivity to contrast material.

5.7 Clinical Application

The most useful application of CTA among intracranial diseases is diagnosis of aneurysms. CTA for intracranial aneurysms is widely used and established. CTA for steno-occlusive diseases is also useful, but it has some limitations. In other vascular diseases such as arteriovenous malformations, dural arteriovenous fistulas, and brain tumors, CTA may be applied as an alternative to MRI/MRA or limited purposes. According to each vascular disease, advantages and limitations of CTA need to be understood.

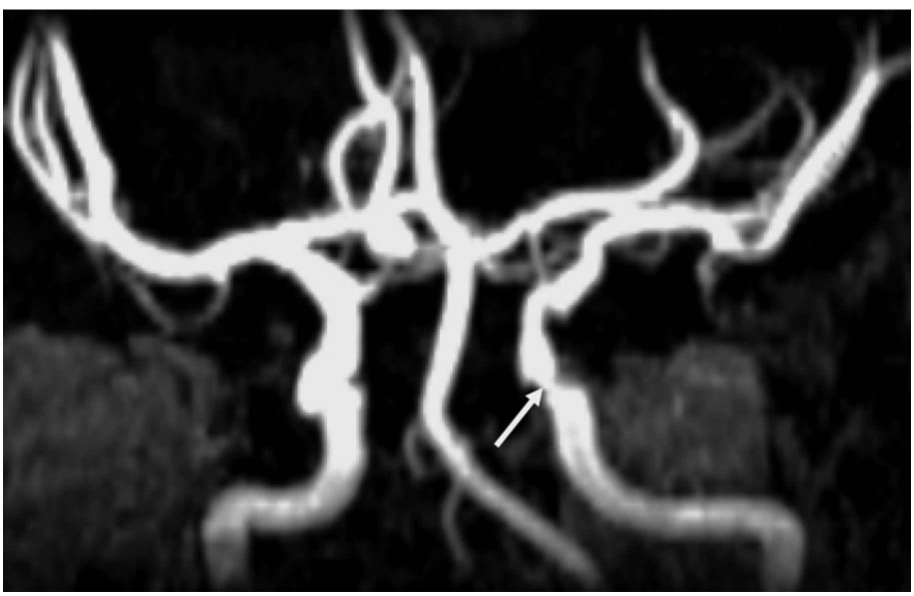

Fig. 5.6 A 48-year-old man with psychiatric problems. Maximum-intensity projection image of MRA from the front shows a stenosis-like area (*arrow*) in the left carotid siphon. The stenosis-like area is caused by artifactual signal loss due to turbulent flow in the carotid siphon.

5.8 Intracranial Aneurysms

5.8.1 Diagnosis and Preoperative Evaluation

Conventional angiography has been considered to be the gold standard for diagnosis and preoperative evaluation of intracranial aneurysms. However, there are several limitations to obtain sufficient information prior to treatment. Superimposition of vessel loops, tortuosity of vessels, small aneurysm size, or complicated aneurysm shape may cause an erroneous detection of an aneurysm or insufficient delineation of the aneurysm and adjacent vessels. To avoid these situations on conventional angiography, different projections, stereoviews, increased magnification, and high frame-rate acquisition may be needed [24]. Also, the limitation of conventional angiography for diagnosis and preoperative study of intracranial aneurysms has been recognized by studies with CTA [4, 5, 25–30] and 3D angiography [31, 32].

The usefulness of CTA for the diagnosis and preoperative evaluation of intracranial aneurysms has been advocated [4, 5, 25–30]. Diagnostic accuracy of CTA is greater for detection of aneurysms larger than 3 mm than for detection of aneurysms 3 mm or smaller [28, 29]. According to previous studies with single-detector helical CT [4, 5, 25–29], the sensitivity and specificity of CTA for intracranial aneurysms larger than 3 mm are 83–100% and 79–100%, and those for intracranial aneurysms 3 mm or less are 51–98% and 79–100%, respectively.

Some authors have suggested that CTA may replace the use of conventional angiography in assessment of acute subarachnoid hemorrhage [25, 26, 30]. In the future, surgery would be performed on the basis of CTA findings alone; however, some limitations in current CTA are considered as follows [27, 28]. First, it requires relatively large amounts of contrast materials and proper timing of the scanning. Second, patient movement due to poor patient condition causes unsatisfactory CT angiographic quality. Third, CTA cannot always be repeated because of risk factors such as renal insufficiency or heart failure. Intravenous injection site and heart function may affect CT angiographic results.

Aneurysms adjacent to the skull base may not always be depicted on CTA. Several authors have described that aneurysms at the skull base that arise from the intracavernous or paraclinoid carotid artery may be obscured by the bone, calcium, or venous blood in CTA studies [25, 26, 28]. The axial source and MPR images of CTA may play an important role in assessing the aneurysms at the intracavernous or paraclinoid carotid artery (Fig. 5.1).

CTA is especially useful for the following conditions: complex-shaped aneurysms, aneurysms with large diameter, thrombosed aneurysms, and complex-overlapping vessels such as the anterior communicating artery aneurysm. Even if carotid angiograms with manual compression of the carotid artery during arteriography are used, DSA does not always clearly depict its presence and the relationship to the anterior communicating artery and bilateral A1 and A2 segments of the anterior cerebral artery in the anterior communicating aneurysm. In thrombosed aneurysm, axial source and MPR images of CTA are useful for assessing the relationship between aneurysm lumen and thrombus within the aneurysm [25] (Fig. 5.3).

Although intraarterial CTA using a combined CT and angiographic unit is a limited method to use, it may be useful for preoperative evaluation of intracranial aneurysms as a supplement to DSA [12]. The additional findings of intraarterial CTA to DSA may affect the following treatment.

5.8.2 Postoperative Follow-up Study

After surgical treatment of an intracranial aneurysm, posttreatment evaluation may be necessary for assessing clipping status. Potential problems include partial clipping of the neck, inadvertent occlusion of vessels after improper clip placement, and migration of the clip. The dome and the neck of the aneurysm after clipping can be evaluated with CTA [33, 34]. CTA is not severely degraded by the presence of nearby aneurysm clips (Fig. 5.7). The very thin collimation of 1 mm or less reduces the severe beam-hardening artifacts seen on routine head studies [33]. CT artifacts may depend on material of the clip [34]. The artifacts caused by the titanium clips are relatively small compared with artifacts from other clips [34].

In the posttreatment evaluation of aneurysm embolization using Guglielmi detachable coils, MRA is a noninvasive useful tool [35–37]. Several reports have described that 3D TOF MRA had high sensitivity with few coil-induced artifacts in detecting residual necks of aneurysms treated with Guglielmi detachable coils. Embolic materials made of platinum seem to have few coil-induced artifacts. Since the platinum coils cause remarkable artifacts on CT, MR studies are more preferable for patients treated with platinum coils than CT studies.

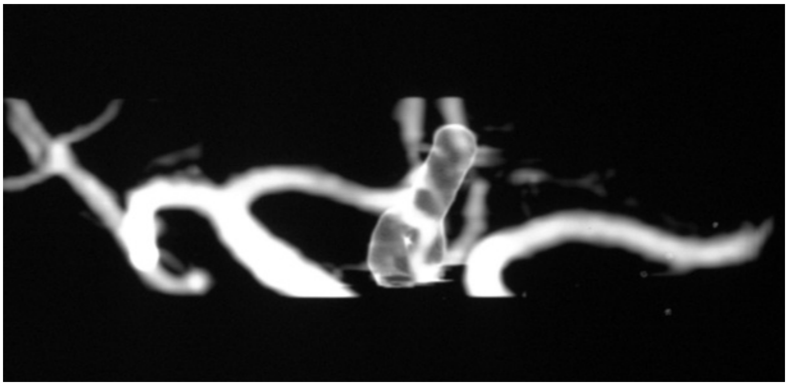

Fig. 5.7 A 52-year-old man with post-surgical clipping of ruptured anterior communicating aneurysm. Volume-rendered CTA image reveals the clip and the adjacent arterial structures. Residual lumen of the aneurysm is not depicted. Contrast angiography also shows no residual lumen of the aneurysm.

5.9 Steno-occlusive Diseases

5.9.1 Atherosclerotic Narrowing

Atherosclerotic narrowing of the major intracranial arteries is associated with the risk of stroke [38]. A warfarin–aspirin symptomatic intracranial disease study showed that symptomatic patients with 50–99% stenosis of an intracranial artery benefited from anticoagulation therapy [39]. Although conventional angiography is a gold standard for evaluating intracranial steno-occlusive diseases, cerebral angiographic complications still remain. Among noninvasive imaging modalities, MRA allows accurate discovery of intracranial steno-occlusive diseases and is widely used as a screening method [40–42]. However, MRA has a potential for consistent overestimation of stenosis. The clinical efficacy of CTA in the evaluation of narrowing of the lumen of the intracranial artery has already been shown to be sensitive and specific [6, 7, 43]. Skutta et al. [44] retrospectively studied the usefulness of CTA for evaluating the intracranial steno-occlusive diseases in 112 patients. They concluded that CTA was a reliable method for grading intracranial steno-occlusive lesions, with the exception of the petrous segment of the carotid artery. Hirai et al. [11] prospectively studied intracranial steno-occlusive diseases with MRA, CTA, and DSA. MRA had a sensitivity of 92%, a specificity of 91%, and an accuracy of 91% for the identification of stenosis of 50% or greater, while additional use of CTA yielded a sensitivity of 100%, a specificity of 99%, and an accuracy of 99% [11]. The combined MRA and CTA provided significantly higher diagnostic accuracy than did MRA alone. The combined evaluation reduced the tendency to overestimate stenosis seen with MRA and improved the specificity for detecting stenosis of 50% or greater. The combined MRA and CTA could achieve equal accuracy to DSA in measuring stenosis and detecting occlusion of the major intracranial arteries in most patients with suspected steno-occlusive diseases [11]. However, CTA may not always correctly delineate the lumen of the artery with circumferential calcification and the cavernous portion of the internal carotid artery [11] (Fig. 5.4).

5.9.2 Acute Embolic Stroke

In patients with large-vessel embolic stroke, intraarterial thrombolytic treatment performed within 6 h of stroke onset can reduce the incidence of disability [45, 46]. Large-vessel stroke may be difficult to distinguish from transient ischemic attacks, lacunar infarctions, postseizure states, peripheral neuropathies, complex migraine, and toxic metabolic encephalopathies [47]. In order to perform effective treatment, it is important to accurately and rapidly detect intracranial steno-occlusive diseases. Knauth et al. [11] prospectively evaluated the usefulness of CTA of the intracranial vessels compared with conventional angiography in 21 patients with acute ischemic stroke. In this study, CTA correctly demonstrated all trunk occlusions of the basilar artery, the internal carotid artery, and the middle cerebral artery. Lev et al. [48] studied 44 consecutive intraarterial candidates who were examined with CTA. Sensitivity and specificity for the detection of large-vessel occlusion were 98.4% and 98.1%, respectively. They concluded that CTA is highly accurate for the detection and exclusion of large-vessel intracranial occlusion and may be valuable in the triage of hyperacute stroke patients to intraarterial thrombolytic treatment.

5.9.3 Moyamoya Disease

Moyamoya disease is a rare cerebrovascular occlusive disease of unknown cause that occurs predominantly in the Japanese, although cases in other ethnic groups have also been described [49, 50]. The angiographic features of this disease include (a) bilateral stenosis or occlusion of the supraclinoid portion of the internal carotid artery (ICA) that extends to the proximal portions of the anterior cerebral artery and the middle cerebral artery, and (b) the presence of parenchymal, leptomeningeal, or transdural collateral vessels that supply the ischemic brain [51, 52]. Although conventional angiography remains the principal imaging technique for demonstrating anatomical changes in detail, less invasive CTA provides an accurate means of diagnosing moyamoya disease when it is suspected on CT, MRI, or clinical grounds [53].

5.9.4 Arterial Dissection

Dissections of the intracranial artery are relatively uncommon vascular diseases that usually affect the supraclinoid carotid, middle cerebral, or vertebrobasilar arteries [54–57]. These lesions have been recognized as a cause of stroke in young and middle-aged adults [54–57].

The accurate diagnosis of intracranial dissections is important for appropriate management of patients. Although conventional angiography is the classic gold standard for the diagnosis of intracranial artery dissection, it rarely demonstrates specific angiographic signs such as a double lumen or intimal flap. Noninvasive imaging techniques including MRI, MRA, and CTA have been reported to be valuable methods for establishing the initial diagnosis and for follow-up studies [58–61].

5.10 Extracranial–Intracranial Bypass

In patients with ischemic cerebrovascular disease, extracranial–intracranial (EC-IC) bypass can be used to improve cerebral blood flow and halt the extension of affected areas or reduce the risk of future strokes, although the effectiveness of this technique remains controversial [62]. The superficial temporal artery–middle cerebral artery anastomosis is frequently performed for the treatment of supratentorial ischemia. In patients with moyamoya disease, encephaloduroarteriosynangiosis and modified encephaloduroarteriosynangiosis procedures have been performed. To examine the patency of EC-IC anastomosis after surgery, conventional cerebral angiography has been the most reliable imaging method among several modalities [63].

CTA using a multidetector CT unit is useful for assessing EC-IC bypass routes [64]. The wide scanning range is valuable for demonstrating the donor and recipient arteries on a single image.

5.11 Arteriovenous Malformation

Intracranial arteriovenous malformations (AVMs) are a complex network of abnormal vascular channels that consists of arterial feeders, the AVM nidus, and venous drainage channels. Cerebral angiography is a gold standard of this disease and can provide the hemodynamic information and the angioarchitecture.

Three-dimensional reconstruction of CTA is very helpful in demonstrating the nidi, drainers, and 3D structure of AVMs [65] (Fig. 5.8). Demonstrations of feeders are not remarkable. CTA of cerebral AVMs could be performed routinely, and 3D imaging is helpful in demonstrating the complex anatomy of cerebral AVMs. This technique may be helpful in planning gamma-knife radiosurgery.

5.12 Carotid-Cavernous Sinus Fistulas

Carotid-cavernous sinus fistulas (CCFs) are classified into dural and direct types. CCFs usually appear as neuro-ophthalmologic symptoms that include proptosis, chemosis, cranial nerve palsies, and dilated episcleral veins.

Although DSA is currently the standard of reference for the diagnosis of dural and direct CCFs, CTA can provide noninvasive diagnosis of these diseases [66]. CTA depicts an enlarged enhancing cavernous sinus and venous drainage channels such as the superior ophthalmic vein, petrosal sinus, sphenoparietal sinus, and intercavernous sinus [66] (Fig. 5.5).

5.13 Brain Tumors

CTA is an alternative method to evaluate extra-axial brain tumors. However, it is not usually applied to intra-axial brain tumors. In large skull base tumors such as meningiomas and pituitary adenomas, CTA may be useful for preoperative evaluation.

5.13.1 Meningiomas

Skull-base meningiomas often involve intracranial vessels. Preoperative evaluation of the tumor is essential for successful surgical removal. Although DSA clearly demonstrates the vascular structure of meningiomas, it does not show the relationship between tumors and bony structures and has a risk of neurological complication. MRA is a noninvasive method that is widely used in the evaluation of patients with meningiomas.

CTA depicts the relationship between skull-base meningiomas and neighboring bony and vascular structures clearly, with minimal risk to the patients [67] (Fig. 5.9).

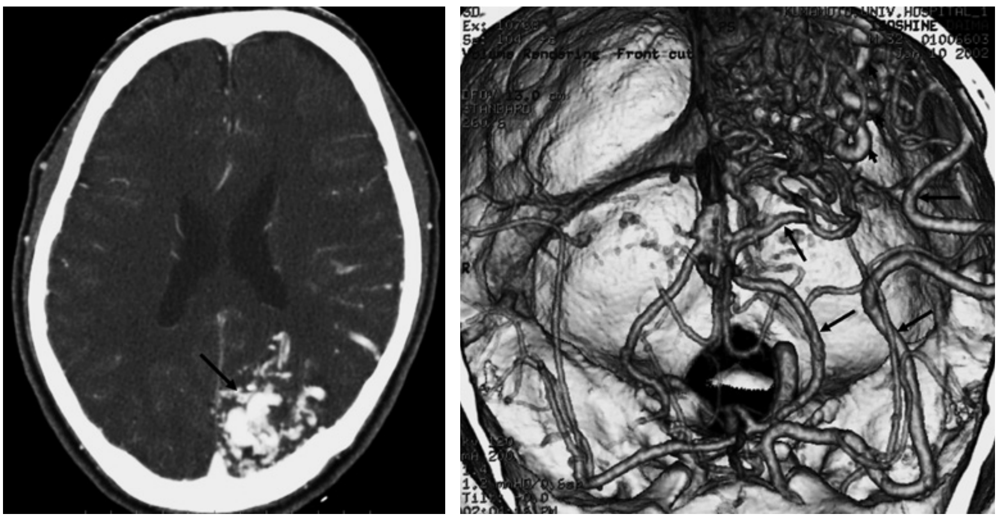

a b

Fig. 5.8a,b A 32-year-old man with left parietooccipital arteriovenous malformation. **a** Contrast-enhanced axial CT image shows abnormal enlarged vessels (*arrow*) in the parietooccipital region, which suggest cerebral arteriovenous malformation. **b** Volume-rendered CTA image from the front and above shows feeding arteries (*arrows*) from the middle and posterior cerebral arteries and draining veins (*arrowheads*).

a b

Fig. 5.9a,b A 67-year-old man with left sphenoid ridge meningioma. **a** Volume-rendered CTA image from the above shows left sphenoid ridge mass (*arrows*) and wall irregularity of the left anterior cerebral artery (*arrowheads*) suggesting tumor encasement. **b** Multiplanar reconstruction image of CTA shows the encasement of the left carotid fork (*arrow*) in the tumor.

References

1. Reyberg J, Buckwalter KA, Caldemeyer KS et al. (2000) Multisection CT: scanning techniques and clinical applications. Radiographics 20:1787–1806
2. Bae KT, Heiken JP, Brink JA (1998) Aortic and hepatic peak enhancement at CT: effect of contrast medium injection rate-pharmacokinetic analysis and experimental porcine model. Radiology 206:455–464
3. Yamashita Y, Komohara Y, Takahashi M et al. (2000) Abdominal helical CT: evaluation of optimal doses of intravenous contrast material-a prospective randomized study. Radiology 216:718–723
4. Hope JKA, Wilson JL, Thomson FJ (1996) Three-dimensional CT angiography in the detection of intracranial berry aneurysms. AJNR Am J Neuroradiol 17:439–445
5. Ogawa T, Okudera T, Noguchi K et al. (1996) Cerebral aneurysms: evaluation with three-dimensional CT angiography. AJNR Am J Neuroradiol 17:447–454
6. Knauth M, Kummer R von, Jansen O et al. (1997) Potential of CT angiography in acute ischemic stroke. AJNR Am J Neuroradiol 18:1001–1010
7. Shrier DA, Tanaka H, Numaguchi Y et al. (1997) CT angiography in the evaluation of acute stroke. AJNR Am J Neuroradiol 18:1011–1020
8. Van Hoe L, Marchal G, Baert AL et al. (1995) Determination of scan delay-time in spiral CT-angiography: utility of a test bolus injection. J Comput Assist Tomogr 19:216–220
9. Hittmair K, Fleischmann D (2001) Accuracy of predicting and controlling time-dependent aortic enhancement from a test bolus injection. J Comput Assist Tomogr 25:287–294
10. Hirai T, Korogi Y, Ono K et al. (2001) Maximum stenosis of extracranial internal carotid artery: effect of luminal morphology on stenosis measurement by using CT angiography and conventional DSA. Radiology 221:802–809
11. Hirai T, Korogi Y, Ono K et al. (2002) Prospective evaluation of suspected stenoocclusive disease of the intracranial artery: combined MR angiography and CT angiography compared with digital subtraction angiography. AJNR Am J Neuroradiol 23:93–101
12. Hirai T, Korogi Y, Ono K et al. (2001) Preoperative evaluation of intracranial aneurysms: usefulness of intraarterial 3D CT angiography and conventional angiography with a combined unit-initial experience. Radiology 220:499–505
13. Ochi T, Shimizu K, Yasuharu Y et al. (1999) Curved planar reformatted CT angiography: usefulness for the evaluation of aneurysms at the carotid siphon. AJNR Am J Neuroradiol 20:1025–1030
14. Kuszyk BS, Heath DG, Ney DR et al. (1995) CT angiography with volume rendering: imaging findings. AJR Am J Roentgenol 165:1579–1580
15. Johnson PT, Heath DG, Kuszyk BS, Fishman EK (1996) CT angiography with volume-rendering: advantages and application in spanchnic vascular imaging. Radiology 200:564–568
16. Davis CP, Ladd ME, Romanowski BJ et al. (1996) Human aorta: preliminary results with virtual endoscopy based on three-dimensional MR imaging data sets. Radiology 199:37–40
17. Rubin GD, Beaulieu CF, Argiro V et al. (1996) Perspective volume rendering of CT and MR images: applications for endoscopic imaging. Radiology 199:321–330
18. Gorzer H, Heimberger K, Schindler E (1994) Spiral CT angiography with digital subtraction of extra and intra cranial vessels. J Comput Assist Tomogr 18:839–841
19. Venema HW, Hulsmans FJH, Heeten GJ den (2001) CT angiography of the circle of Willis and intracranial internal carotid arteries: maximum intensity projection with matched mask bone elimination-feasibility study. Radiology 218:893–898
20. Jayakrishnan VK, White PM, Aitken D et al. (2003) Subtraction helical CT angiography of intra- and extracranial vessels: technical considerations and preliminary experience. AJNR Am J Neuroradiol 24:451–455
21. Remonda L, Senn P, Barth A et al. (2002) Contrast-enhanced 3D MR angiography of the carotid artery: comparison with conventional digital subtraction angiography. AJNR Am J Neuroradiol 23:213–219
22. Heiserman JE, Drayer BP, Keller PJ, Fram EK (1992) Intracranial vascular stenosis and occlusion: evaluation with three-dimensional time-of-flight MR angiography. Radiology 185:667–673
23. Fürst G, Hofer M, Sitzer M et al. (1995) Factors influenceing flow induced signal loss in MR angiography: an in vitro study. J Comput Assist Tomogr 19:692–699
24. Setton A, Davis AJ, Bose A, Nelson PK, Berenstein A (1996) Angiography of cerebral aneurysms. Neuroimag Clin North Am 6:705–738
25. Alberico RA, Patel M, Casey S et al. (1995) Evaluation of the circle of Willis with three-dimensional CT angiography in patients with suspected intracranial aneurysms. AJNR Am J Neuroradiol 16:1571–1578
26. Zouaoui A, Sahel M, Marro B et al. (1997) Three-dimensional computed tomographic angiography in detection of cerebral aneurysms in acute subarachnoid hemorrhage. Neurosurgery 41:125–130
27. Velthuis BK, Rinkel GJE, Ramos LMP et al. (1998) Subarachnoid hemorrhage: aneurysm detection and preoperative evaluation with CT angiography. Radiology 208:423–430
28. Korogi Y, Takahashi M, Katada K et al. (1999) Intracranial aneurysms: detection with three-dimensional CT angiography with volume rendering-comparison with conventional angiographic and surgical findings. Radiology 211:497–506
29. White PM, Wardlaw JM, Easton V (2000) Can noninvasive imaging accurately depict intracranial aneurysms? Systematic review. Radiology 217:361–370
30. Velthuis BK, Leeuwen MS van, Witkamp TD et al. (1999) Computerized tomography angiography in patients with subarachnoid hemorrhage: from aneurysm detection to treatment without conventional angiography. J Neurosurg 91:761–767
31. Hochmuth A, Spetzger U, Schumacher M (2002) Comparison of three-dimensional rotational angiography with digital subtraction angiography in the assessment of ruptured cerebral aneurysms. AJNR Am J Neuroradiol 23:1199–1205
32. Sugahara T, Korogi Y, Nakashima K et al. (2002) Comparison of 2D and 3D digital subtraction angiography in evaluation of intracranial aneurysms. AJNR Am J Neuroradiol 23:1545–1552
33. Vieco PT, Morin III EE, Gross CE (1996) CT angiography in the examination of patients with aneurysm clips. AJNR Am J Neuroradiol 17:455–457

34. Van Loon JJ, Yousry TA, Fink U et al. (1997) Postoperative spiral computed tomography and magnetic resonance angiography after aneurysm clipping with titanium clips. Neurosurgery 41:851–856
35. Derdeyn CP, Graves VB, Turski PA, Masaryk AM, Strother CM (1997) MR angiography of saccular aneurysms after treatment with Guglielmi detachable coils: preliminary experience. AJNR Am J Neuroradiol 18:279–286
36. Kähärä VJ, Seppänen SK, Ryymin PS, et al. (1999) MR angiography with three-dimensional time-of-flight and targeted maximum-intensity-projection reconstructions in the follow-up of intracranial aneurysms embolized with Guglielmi detachable coils. AJNR Am J Neuroradiol 20:1470–1475
37. Weber W, Yousry TA, Felber SR et al. (2001) Noninvasive follow-up of GDC-treated saccular aneurysms by MR angiography. Eur Radiol 11:1792–1797
38. Sacco RL, Kargman DE, Gu Q, Zamanillo MC (1995) Race-ethnicity and determinants of intracranial atherosclerotic cerebral infarction. The Northern Manhattan Stroke Study. Stroke 26:14–20
39. Chimowitz MI, Kokkinos J, Strong J et al. (1995) The warfarin-aspirin symptomatic intracranial disease study. Neurology 45:1488–1493
40. Heiserman JE, Drayer BP, Keller PJ, Fram EK (1992) Intracranial vascular stenosis and occlusion: evaluation with three-dimensional time-of-flight MR angiography. Radiology 185:667–673
41. Korogi Y, Takahashi M, Mabuchi N et al. (1994) Intracranial vascular stenosis and occlusion: diagnostic accuracy of three-dimensional, Fourier transform, time-of-flight MR angiography. Radiology 193:187–193
42. Korogi Y, Takahashi M, Nakagawa T et al. (1997) Intracranial vascular stenosis and occlusion: MR angiographic findings. AJNR Am J Neuroradiol 18:135–143
43 Katz DA, Marks MP, Napel SA, Bracci PM, Roberts SL (1995) Circle of Willis: evaluation with spiral CT angiography, MR angiography, and conventional angiography. Radiology 195:445–449
44. Skutta B, Fürst G, Eilers J et al. (1999) Intracranial steno-occlusive disease: double-detector helical CT angiography versus digital subtraction angiography. AJNR Am J Neuroradiol 20:791–799
45. Del Zoppo G, Higashida R, Furlan A et al. (1998) PROACT: a phase II randomized trial of recombinant pro-urokinase by direct arterial delivery in acute middle cerebral artery stroke. PROACT Investigators. Prolyse in acute cerebral thromboembolism. Stroke 29:4–11
46. Furlan A, Higashida R, Wechsler L et al. (1999) Intra-arterial prourokinase for acute ischemic stroke. The PROACT II study: a randomized controlled trial. Prolyse in acute cerebral thromboembolism. JAMA 282:2003–2011
47. Libman R, Wirkowski E, Alvir J et al. (1995) Conditions that mimic stroke in the emergency department. Implications for acute stroke trials. Arch Neurol 52:1119–1122
48. Lev MH, Farkas J, Rodriguez VR et al. (2001) CT angiography in the rapid triage of patients with hyperacute stroke to intraarterial thrombolysis: accuracy in the detection of large vessel thrombus. J Comput Assist Tomogr 25:520–528
49. Suzuki J, Takaku A (1969) Cerebrovascular "moyamoya" disease: disease showing abnormal net-like vessels in base of brain. Arch Neurol 20:288-299
50. Taveras JM (1969) Multiple progressive intracranial arterial occlusions: a syndrome of children and young adults. AJR 106:235–268
51. Takahashi M (1980) Magnification angiography in moyamoya disease: new observations on collateral vessels. Radiology 136:379–386
52. Yamada I, Himeno Y, Suzuki S, Matsushima Y (1995) Posterior circulation in moyamoya disease: angiographic study. Radiology 197:239–246
53. Tsuchiya K, Makita K, Furui S (1994) Moyamoya disease: diagnosis with three-dimensional CT angiography. Neuroradiology 36:432–434
54. Hart RG, Easton JD (1983) Dissections of cervical and cerebral arteries. Neurol Clin 1:155–182
55. Caplan LR, Baquis GD, Pessin MS et al. (1988) Dissection of the intracranial vertebral artery. Neurology 38:868–877
56. Provenzale JM (1995) Dissection of the internal carotid and vertebral arteries: imaging features. AJR Am J Roentgenol 165:1099–1104
57. Shievink WI (2001) Spontaneous dissection of the carotid and vertebral arteries. N Engl J Med 344:898–906
58. Hosoya T, Watanabe N, Yamaguchi K, Kubota H, Onodera Y (1994) Intracranial vertebral artery dissection in Wallenberg syndrome. AJNR Am J Neuroradiol 15:1161–1165
59. Hirai T, Korogi Y, Murata Y et al. (2003) Intracranial artery dissections: serial evaluation with MR Imaging, MR angiography, and source images of MR angiography. Radiat Med 21:86–93
60. Lanzino G, Kaptain G, Kallmes DF, Dix JE, Kassell NF (1997) Intracranial dissecting aneurysm causing subarachnoid hemorrhage: the role of computerized tomographic angiography and magnetic resonance angiography. Surg Neurol 48:477–481
61. Leclerc X, Lucas C, Godefroy O, et al. (1998) Helical CT for the follow-up of cervical internal carotid artery dissections. AJNR Am J Neuroradiol 19:831–837
62. EC-IC Bypass Study Group (1985) Failure of extracranial-intracranial arterial bypass to reduce the risk of ischemic stroke. Results of an international randomized trial. N Engl J Med 313:1191–2000
63. Jack CR Jr, Sundt TM Jr, Fode NC et al. (1988) Superficial temporal-middle cerebral artery bypass: clinical pre- and postoperative angiographic correlation. J Neurosurg 69:46–51
64. Tsuchiya K, Aoki C, Katase S et al. (2003) Visualization of extracranial-intracranial bypass using multidetector-row helical computed tomography angiography. J Comput Assist Tomogr 27:231–234
65. Aoki S, Sasaki Y, Machida T et al. (1998) 3D-CT angiography of cerebral arteriovenous malformations. Radiat Med 16:263–271
66. Coskun O, Hamon M, Catroux G et al. (2000) Carotid-cavernous fistulas: diagnosis with spiral CT angiography. AJNR Am J Neuroradiol 21:712–716
67. Tsuchiya K, Hachiya J, Mizutani Y, Yoshino A (1996) Three-dimensional helical CT angiography of skull base meningiomas. AJNR Am J Neuroradiol 17:933–936